RSC Advances

Highly-sensitive label-free immunosensor for tumor necrosis factor α based on Ag@Pt core-shell nanoparticles supported on MWCNT as efficient electrocatalyst nanocomposite

Journal:	*RSC Advances*
Manuscript ID:	RA-ART-05-2015-008016.R1
Article Type:	Paper
Date Submitted by the Author:	06-Jul-2015
Complete List of Authors:	mazloum, mohammad; Yazd University, Department of Chemistry Hosseinzadeh, Laleh; yazd university,

Highly-sensitive label-free immunosensor for tumor necrosis factor α based on Ag@Pt core-shell nanoparticles supported on MWCNT as efficient electrocatalyst nanocomposite

Mohammad Mazloum-Ardakani*, Laleh Hosseinzadeh

Department of Chemistry, Faculty of Science, Yazd University, Yazd, 89195-741, Iran

E-Mail: mazloum@yazd.ac.ir

Phone No: 00983518211670

Fax No: 00983518210644

Mohammad Mazloum-Ardakani

E-Mail: mazloum@yazd.ac.ir

Phone No: 00983518211670

Fax No: 00983518210644

Laleh Hosseinzadeh

E-Mail: l.hosseinzadeh2011@gmail.com

Highly-sensitive label-free immunosensor for tumor necrosis factor α based on Ag@Pt core-shell nanoparticles supported on MWCNT as efficient electrocatalyst nanocomposite

Mohammad Mazloum-Ardakani*, Laleh Hosseinzadeh

Department of Chemistry, Faculty of Science, Yazd University, Yazd, 89195-741, Iran

E-Mail: mazloum@yazd.ac.ir

Phone No: 00983518211670

Fax No: 00983518210644

ABSTRACT

We have developed a novel and label-free electrochemical immunosensor for detection of tumor necrosis factor-alpha (TNF-α) based on bimetallic silver@platinum (Ag@Pt) core-shell nanoparticles supported on MWCNTs and chitosan (Ag@Pt-CNTs-CS) as a desirable sensor platform. The redox reaction of catechol on the graphite screen-printed electrodes modified with Ag@Pt-CNTs-CS applied as a probe for studying the immobilization and determination processes in immunosensor, due to enhanced electrocatalytic activity of Ag@Pt-CNTs for catechol. The results showed that these nanocomposite exhibited attractive electrocatalytic activity and also yielded large capacity for antibody loading, which improve the amount of immobilized antibody. A decrease in differential pulse voltammetry (DPV) responses was observed with increasing concentrations of TNF-α in standard and real sample due to its obstruction to the electrocatalytic oxidation of catechol by Ag@Pt-CNTs after binding to the surface of electrode through interaction with the antibody. The detection limit for TNF-α was found to be 1.6 pg/mL and the detection concentrations were in the range between 6.0 and 60 pg/mL. The proposed electrochemical immunosensor showed high sensitivity, specificity, good reproducibility and stability as well as acceptable accuracy for TNF-α detection in human serum samples and this strategy might also be applied to detect the other antigens.

Keywords: Silver@platinum core-shell, Electrochemical Immunosensor, Electrocatalytic, Tumor necrosis factor α, Catechol

1. Introduction

Tumor necrosis factor-alpha antigen (TNF-α) is a kind of critical cytokines, regulatory proteins which are secreted by cells of the immune system and act as intercellular mediators in the generation of an immune response, which have been correlated to many infectious and inflammatory diseases such as rheumatoid arthritis, diabetes, stroke, HIV infection, neonatal listeriosis, systemic erythema nodosum leprosum, endotoxic shock, severe meningococcemia and graft rejection [1,2]. Generally, the concentration of biomarkers such as TNF-α in human fluid including blood, urine and other tissues is very low, therefore, determination of biomarkers is very importance because it helps to early diagnosis of diseases, and also provides the possibility of better treatment of diseases. Therefore, the development of high sensitive methods for the detection of biomarkers is of great importance for clinical diagnosis and research.

Electrochemical immunoassays compared with the conventional methods play an increasingly important role in the detection of biomarkers because they have great potential to satisfy the practical need for rapid, portable, high sensitivity and low cost detection [3–7]. Many different electrochemical methods were used in order to fabrication of immunosensor and detection of biomarkers. These methods are mainly based on electrochemical impedance spectroscopy (EIS)[8–10], cyclic voltammetry (CV)[11–13], differential pulse voltammetry (DPV)[14,15] or potentiodynamic techniques [16,17]. The potentiodynamic technique most suitable for the formation of stabile conducting polymer layer for immunosensor application that allow significant enrichment of polymer layer by entrapped biological compound (e.g. enzyme, antibody, single stranded DNA, etc.).[18] Ramanavicius et al.[16] presented a strategy for preparing an amperometric immunosensor for gp51 based on entrapped of immobilized antigens during polymerization within polypyrrole layer. The immunosensor was prepared by pulsed potential

based electrochemical polymerization and analytical signal of this was evaluated by mean of pulsed amperometric detection.

Recently, label-free immunosensors as one of electrochemical immunosensors, which interactions between antibody and antigen are directly monitored without the presence of any labels, have been developed due to their remarkable advantages such as simple fabrication, low cost and fast response. The development of label-free electrochemical immunosensors based on fixed species with electrocatalytic activity on the surface of electrodes is also considerable that can increase sensitivity of label-free immunosensors [19–22].

Multiwall carbon nanotubes (MWCNTs) have been widely used in fabrication of biosensors because of unique physical, chemical and electronic properties such as chemical inertness, low residual current, excellent conductivity, wide potential window, and high surface area [23–25]. Since bimetallic nanoparticles show interesting catalytic, optical, electronic and magnetic properties than from the corresponding monometallic particles, recently, they have received significant attention. The catalytic activity of metallic nanoparticles is strongly dependent on the shape and size and aggregation of these nanoparticles can decrease their catalytic activity. The suitable supports for nanoparticles such as MWCNTs offer high surface area for distribution more number of nanoparticles for immobilizing of biomolecules and avoid aggregation of them, thereby improving the catalytic, optical, electronic and magnetic properties of metallic nanoparticles [26–28]. According to the above points, silver@platinum core-shell supported on MWCNTs (Ag@Pt-CNTs) provides a nanocomposite by good selectivity, high stability and superior catalytic properties which increase the amplification of electrochemical signals and apply to high sensitive detection of TNF-α.

In the present work, we have developed a desirable platform based on Ag@Pt core-shell nanoparticles supported on MWCNTs and chitosan (Ag@Pt-CNTs/CS) as a nanocomposite for the fabrication of highly-sensitive label-free electrochemical immunosensors for enzyme-free determination of TNF-α biomarker. The present results demonstrate that the Ag@Pt-CNTs nanocomposite has remarkably electrocatalytic activity towards the oxidation of catechol (1,2-dihydroxy-benzene), therefore, catechol applied as a probe in immunosensor. This immunosensor fabrication strategy is simple and rapid, that may provide many potential applications for the sensitive detection of different biomarkers.

2. Experimental

2.1. Materials

Chloroplatinic acid solution (8 wt. % in H_2O), ethanolamine, silver nitrate and ethylene glycol (EG) were purchased from Sigma-Aldrich. Catechol, sodium borohydride, trisodium citrate, sodium hydroxide, sodium dihydrogen phosphate, disodium hydrogen phosphate, potassium ferrocyanide ($K_4[Fe(CN)_6]$), potassium ferricyanide ($K_3[Fe(CN)_6]$), acetic acid and chitosan were obtained from Merck. Multiwalled carbon nanotubes (purity more than 95%) with o.d. between 5 and 20 nm, i.d. between 2 and 6 nm, and tube length 1–10 μm were purchased from plasma Chem (Germany). The immunologic reagents TNF-α antibody (anti-TNF-α, Ab) and TNF-α antigen (Ag) were obtained from Abcam (Cambridge, UK). Bovine serum albumin (BSA, Equitech-Bio, USA) was used as a specific control. Fresh human plasma samples were supplied by a local hospital (Shahid Sadoughi hospital, Yazd, Iran). All experiments were

performed in compliance with the relevant laws and institutional guidelines, and the Medical Research Ethics Board of Yazd University has approved for this experiments.

2.2. Instrumentation

The electrochemical measurements were performed with an Autolab potentiostat/galvanostat (PGSTAT-302 N, Eco Chemie, Netherlands). The experimental conditions were controlled with General Purpose Electrochemical System (GPES) and Frequency Response Analyzer (FRA) software. Graphite screen-printed electrodes (SPEs) with graphite working electrode, a graphite counter electrode and a silver pseudo-reference electrode were purchased from Palm instruments BV (Netherlands). All the functionalization steps involved in the assembly of the immunosensor were performed using 8 μL of the appropriate solution deposited on the graphite screen-printed working electrode surface in order to prevent the fouling of counter and reference screen-printed electrodes.

Ultraviolet–Visible (UV–Vis) spectra were obtained by an Optizen 3220 UV–Vis spectrophotometer.

2.3. Preparation of Ag@Pt-CNTs/CS nanocomposites

Ag@Pt-CNTs were prepared according to the previous report [27]. In brief, the preparation of Ag@Pt-CNTs nanocomposite was according to the following steps: First, MWCNTs were purified by using acid treatment. Then, 5 mg of MWCNT powder was dispersed in 10 mL of $AgNO_3$ aqueous solution (0.5 mM) with sonication for 1 h. Subsequently, this solution was mixed with 80 μL of 19.4 mM aqueous sodium citrate solution (used as a stabilizer). Second, 1 mL of 11.2 mM aqueous sodium borohydride solution was added dropwise under vigorous

stirring, giving rise to a yellow solution. Third, the obtained solution was centrifuged and dried at 80°C in a vacuum oven. Then, powder product was dispersed in 1 ml of EG/H_2O mixture with volume ratio of 1:1 by sonication. Afterwards, 37.5 μL of chloroplatinic acid solution was added and the pH of the mixture was adjusted to 8.0 by adding KOH/EG/H_2O solution. After the mixture was stirred for 4 h at 90°C, the product nanocomposite was centrifuged and washed eight times with water and dried at 80°C in a vacuum oven for 24 h. Finally, 1 mg of Ag@Pt-CNTs nanocomposite obtained was redispersed in 1.5 mL CS solution (0.1% in 1% of acetic acid) by sonication for 1 h.

2.4. Preparation of the immunosensor

Scheme 1 shows the fabrication procedure of the proposed electrochemical immunosensor. 5 μL of Ag@Pt-CNTs/CS nanocomposite suspension was dropped onto the screen-printed working electrode surface in order to prevent the fouling of counter and reference screen-printed electrodes and drying at room temperature. Afterward, 8 μL of 40 ppm anti-TNF-α was placed on the modified electrode for 6 h at 4°C and then washed with PBS buffer (pH=7.4) to remove unspecific physically adsorption. After incubation of anti-TNF-α, the remaining non-specific active sites on working electrode were blocked by ethanolamine solution (8 μL, 10 mM) for 0.5 h. Theas-prepared immunosensor (designed as SPE/Ag@Pt-CNTs/CS/Ab) was used for detection of TNF-α during the experiment.

For the determination of TNF-α, the immunosensor was washed thoroughly with PBS buffer and incubated with a varying concentration of TNF-α for overnight at 4°C, and subsequently the electrode was rinsed thoroughly to eliminate possible unstable adsorbed TNF-α from the electrode surface. Electrochemical measurements of this immunosensor toward TNF-α

samples or standards were carried out through 1 mM catechol (prepared in 0.1 M PBS (pH 7.4)) as a probe. The Ag@Pt-CNTs/CS modified electrode was directly used for immobilizing antibody. After adding TNF-α antigen, it will form complexes with antibody; therefore, covered the surface of Ag@Pt-CNTs/CS modified electrode and blocked the catalysis effect of Ag@Pt-CNTs to the oxidation of catechol. The current response in DPV, from 0.0 to 0.2 V with a pulse amplitude of 50 mV and a pulse width of 20 ms) decreased with the increase of TNF-α concentration. The decrease of DPV peak current is proportion to the increasing concentrations of TNF- α, which will use to determination of TNF-α.

Here Scheme 1

3. Results and discussion

3.1. Characterization of Ag@Pt-CNTs nanocomposite

The Ag@Pt-CNTs nanocomposite was characterized by TEM and UV-Vis absorption. The response of a nanocomposite on electrode surface is related to its physical morphology. Fig. 1A shows the TEM image of the Ag@Pt-CNTs. The good distribution and the small size of Ag@Pt core-shell nanoparticles on MWCNTs are the effective factors on catalytic activity of them; on the other hand, MWCNTs were excellent disperser which inhibited the aggregation of Ag@Pt core-shell nanoparticles. The MWCNTs as a suitable supports and stabilizer offer high surface area for better distribution and avoid aggregation of them, therefore, the Ag@Pt-CNTs should have very good performance and stability in this immunosensor [26,28]. The uniform distribution of Ag@Pt core-shell nanoparticles on the MWCNT could be observed. We have further

investigated the synthesized Ag nanoparticles-MWCNT by using UV-vis absorption spectroscopy to explore of the respective synthesis. As shown in Fig. 1B, the results of our UV-vis absorption spectroscopic studies of Ag nanoparticles synthesized in the absence and presence of MWCNTs indicate the synthesized Ag nanoparticles have been decorate on the MWCNTs. The absorption peak of Ag nanoparticles was decreased when synthesized in the presence of MWCNTs; it proved that Ag nanoparticles decorated on the MWCNTs.

The oxygenated functional groups formed on the acid-treated MWCNTs surface which has negative charge are activated positions for adsorption of the Ag cations in solution because of electrostatic interactions and then these ions could be reduced by the addition of reducing agent [29,30]. On the other hand, it is confirmed that there are two reasons for the coverage of Ag nanoparticles by Pt and formation of the core-shell structure: first, the interaction between the metals is stronger than that between metal and carbon; second, Pt and Ag crystallites have face-centered cubic structure, which is in favor of the growth of Pt in the Ag nanoparticles surface [27,31]. Therefore, Ag@Pt core-shell nanoparticles supported on MWCNTs was synthesized as a nanocomposite by unique properties which increase the amplification of electrochemical signals and apply to high sensitive detection of biomarker.

Here Fig. 1

3.2. The electrochemical characterization of the modified electrodes

A label-free immunosensor for the enzyme-free detection of TNF-α was prepared by modified SPEs with the Ag@Pt-CNTs/CS nanocomposite which has good electrocatalytic activity for the oxidation of catechol. According to the precise, rapid and simple enzyme-free

oxidation of catechol, it is very important in usage of catechol as a probe in electrochemical biosensors. The enzymes require specific experimental conditions such as pH, toxic chemicals and temperature which are inherently instable over time. Therefore, enzyme-free sensors are more trustworthy in long-time [32]. The Ag@Pt core-shell nanoparticles in Ag@Pt-CNTs/CS nanocomposite presented numerous possibilities for coupling of antibody under reaction conditions. The antibody-coated SPE then was used to capture TNF-α from the TNF-α containing solution. This assay was characterized by CV and EIS.

Cyclic voltammograms of the probe are valuable and convenient tools to monitor the barrier of the modified electrode, because the electron transfer between the solution species and the electrode must occur by tunneling either through the barrier or through the defects in the barrier. Therefore, it was chosen as a marker to investigate the changes of electrode behavior after each assembly step [33]. Inset of Fig. 2 shows typical cyclic voltammograms of different electrodes in 1.0 mM catechol in 0.1 M PBS (pH 7.4) at a scan rate of 100 mV/s. A pair of well-defined redox peaks is observed at the bare SPE (curve a, Inset of Fig. 2). To investigate the roles of Ag@Pt core-shell nanoparticles on electrochemical response of nanocomposite, the CVs at the Ag@Pt-CNTs/CS modified SPE (curve c Inset of Fig. 2) and CNTs/CS modified SPE (curve b Inset of Fig. 2) were recorded. The results indicated that the presence of Ag@Pt core-shell nanoparticles on MWCNTs in nanocomposite exhibited great improvement on the peak current, which indicated that the Ag@Pt core-shell nanoparticles on MWCNTs improved the electrocatalytic activity of nanocomposite for oxidation of catechol. When antibody was conjugated onto the modified SPE through the interaction between the amino groups of antibody and Ag@Pt core-shell nanoparticles [34,35], the peak current decreased which suggested that the formation of insulating layers of proteins, perturbs the interfacial electron transfer considerably

and prevents the electrocatalytic oxidation of catechol (curve d, Fig. 2). After TNF-α (15 pg mL^{-1}) was immobilized on the electrode, there is another decrease of peak current, indicating the formed complex between antibody and TNF-α acted as the electron-transfer blocking layer, which greatly inhibited the reaction on the electrode surface (curve e, Fig. 2). From these results, it could be seen that the Ag@Pt-CNTs/CS modified SPE with its electrocatalytic effect on oxidation of catechol could be used for the detection of TNF-α by a label-free and enzyme-free immunosensor. Also, this significant change in the CV curve after immobilization of antibody and TNF-α onto the modified electrode surface, indicates an efficient bonding of them over the modified electrode surface. Inset of Fig. 2 shows typical cyclic voltammograms of different electrodes in buffer solution (pH = 7.4). As expected the capacitance current value at the Ag@Pt-CNTs/CS modified SPE (curve g) is greater than bare SPE (curve f) which due to the accessible capacitance of the Ag@Pt-CNTs/CS at the SPE [36].

Here Fig. 2

The EIS method was effective to probing the feature of the surface, which could be used as a parameter to understand the chemical transformations and processes associated with the conductive surface [37]. Fig. 3 shows the Nyquist plots of EIS corresponding to the fabrication of immunosensors after each step. The semicircle diameters of Nyquist plot reflect the electron transfer resistance (R_{ct}), which is related to the electron transfer kinetics of the redox probe at the surface of the electrode [38]. Here, Nyquist plot of bare SPE showed as curve a in inset of Fig. 3.

It could be seen that on the Ag@Pt-CNTs/CS (curve c) the value of R_{ct} is smaller than to CNTs/CS (curve b), which was due to the excellent electrical property of Ag@Pt core-shell nanoparticles that formed a high electron conduction pathway between the electrode and electroactive indicator. Subsequently, when the antibody was immobilized on the modified electrode, the inter-facial resistance increased (Fig. 3, curve d). The result indicated that the protein layer on the electrode generated a barrier for electron-transfer, which was similar to the previous report [3]. Similarly, R_{ct} further increased with the assembled of TNF-α (curve e) on the modified electrode above, because the additions resist the electron-transfer kinetics of the redox probe at the electrode interface. These results are in conformity to a similar pattern of results obtained with CVs measurements, which further confirms the fabrication of this immunosensor. The EIS spectra are fitted to the equivalent circuit as shown in Fig. S1[39]. Equivalent circuits used for data interpretation are shown for bare electrode in Fig. S1A; for SPE/CNTs/CS and SPE/Ag@Pt-CNTs/CS in Fig. S1B; for SPE/Ag@Pt-CNTs/CS/Ab and SPE/Ag@Pt-CNTs/CS/Ab/Ag in Fig. S1C.

Here Fig. 3

3.3. Optimization of the experimental parameters

To obtain the best conditions in the preparation of the SPE/Ag@Pt-CNTs/CS/Ab, we optimized the effective parameters such as concentration and incubation time of antibody, incubation time of TNF-α and concentration of catechol. In this work, CV and EIS spectra were employed to characterize the interface properties of surface modified electrodes.

The incubation time of antibody was experimentally investigated; according to the results, 6 h is the optimum incubation time (Fig. S2A). As illustrated with increasing incubation time from 1 h to 6 h the immunosensor response increased, then starts to level off, therefore 6 h was used as optimum incubation time. Moreover, the concentration of antibody has great effects on sensitivity of immunosensor. Therefore, different concentrations of antibody solution (20, 40 and 60 ppm) were used to optimize the immunosensor concentration (Fig. S2B). Then, Nyquist plots of EIS were recorded for different concentrations of antibody on modified electrode and highest sensitivity was observed when antibody solution of 40 ppm was used. Similarly, the effect of the incubation times of TNF-α on sensitivity of immunosensor were also investigated and optimum times of overnight was selected (Fig. S2C). In the above, EIS measurements were employed to optimize conditions by using 10 mM $[Fe(CN)_6]^{3-/4-}$ redox probe prepared in 0.1 M KCl and 0.1 M PBS pH 7.4.

The electrocatalytic activity of Ag@Pt-CNTs/CS modified SPE towards the oxidation of catechol with different concentrations was investigated by CVs (Fig. S2D). As shown in Fig. S2D, it can be obviously found that the currents increase with increasing concentrations of catechol to 1 mM. Therefore, 1 mM of catechol was chosen as the optimum concentration.

3.4. Performance of the immunosensor

In order to quantitatively evaluate the sensitivity and dynamic range of the immunosensor, the calibration curve of the immunosensor to various concentrations of TNF-α was obtained by DPV technique. As expected, the DPV currents of the immunosensor decreased with the increasing concentrations of TNF-α, and exhibited a good linear relationship with the TNF-α concentration from 6.0 to 60.0 pg mL^{-1} (Fig. 4). The linear regression equation was adjusted to $I\,(\mu A) = +55.43 - 0.37[\mathrm{TNF} - \alpha](\mathrm{pg\,mL^{-1}}, R^2 = 0.9983)$, with a detection limit (LOD) of 1.6

pg mL^{-1}at a signal-to-noise ratio of 3σ (where σ is the standard deviation of the blank, n = 10). Compared with the other immunosensors in literature, the fabricated immunosensor has high sensitivity (Table S1).

Here Fig. 4

3.5. Reproducibility, stability and selectivity of the immunosensor

Since reproducibility is a very important characteristic for the real application of the sensors, it was necessary to investigated. Five different immunosensors were prepared independently at the same experimental condition and tested for the detection of the same concentration of TNF-α. The relative standard deviations (RSD) of 2.6 % and 2.23% were obtained for the detection of 15.0 pg mL^{-1} and 60.0 pg mL^{-1} of TNF-α, respectively. These results suggested the acceptable fabrication reproducibility and precision of the immunosensor. Stability of this immunosensor is a key factor in their application and development. The long time stability of the immunosensor was also investigated by storing it in 4℃ in refrigerator. The response of the immunosensor for 15.0 pg mL^{-1} of TNF-α after 20 days was about 95% of its initial response.

The specificity of the TNF-α immunosensor was evaluated as an important criterion for analytical methods. The signal values for BSA at a concentration of 60 pg mL^{-1} in the presence of 15 pg mL^{-1} of TNF-α was used as an indicator for the selectivity of the sensor in comparison with the TNF-α alone. The ratios of currents with interfering substance (BSA) to pure TNF-α were 1.07. The results showed that negligible interference was observed under the experimental conditions.

3.6. Application of the immunosensor in human serum

In order to demonstrate the practical application of the immunosensor for clinical diagnosis, the recovery test was performed. Different concentrations of TNF-α were added into the human serum and then detected by the immunosensor. The percent of TNF-α detected by the immunosensor from these serum samples indicating the reliability of the detection results (Table 1).

Here Table 1

4. Conclusion

In summary, we have developed a new and high sensitive label-free electrochemical immunosensor based on Ag@Pt-CNTs/CS nanocomposite modified SPEs for enzyme-free determination of TNF-α biomarker, which showed good linear ranges (6.0 to 60.0 pg mL^{-1}) and low detection limits (1.6 pg mL^{-1}). Catechol introduced as a probe in this work due to remarkably electrocatalytic activity of Ag@Pt-CNTs nanocomposite towards the oxidation of catechol. The approach provided a convenient, high sensitive, simple and rapid method for TNF-α detection, which might provide many potential applications for the high sensitive detection of different biomarkers.

Acknowledgements

The authors wish to thank the Yazd University Research Council, the IUT Research Council and Excellence in Sensors for financial support of this research.

References

1 S. de Kossodo, V. Houba and G. E. Grau, *J. Immunol. Methods*, 1995, **182**, 107–114.

2 S. Galic, J. S. Oakhill and G. R. Steinberg, *Mol. Cell. Endocrinol.*, 2010, **316**, 129.

3 M. Mazloum-Ardakani, L. Hosseinzadeh and Z. Taleat, *Microchim. Acta*, 2014, **161**, 917–924.

4 S. Samanman, A. Numnuam, W. Limbut, P. Kanatharana and P. Thavarungkul, *Anal. Chim. Acta*, 2015, **853**, 521–532.

5 M. Mazloum-Ardakani and A. Khoshroo, *Anal. Chim. Acta*, 2013, **798**, 25–32.

6 Z. Taleat, A. Khoshroo and M. Mazloum-Ardakani, *Microchim. Acta*, 2014, **161**, 865–891.

7 S. Zhang, Y. Wang, Y. Zhang, T. Yan, L. Yan, Q. Wei and B. Du, *RSC Adv.*, 2015, **5**, 6512–6517.

8 P. Kongsuphol, H. H. Ng, J. P. Pursey, S. K. Arya, C. C. Wong, E. Stulz and M. K. Park, *Biosens. Bioelectron.*, 2014, **61**, 274–279.

9 J. T. La Belle, K. Bhavsar, A. Fairchild, A. Das, J. Sweeney, T. L. Alford, J. Wang, V. P. Bhavanandan and L. Joshi, *Biosens. Bioelectron.*, 2007, **23**, 428–431.

10 T. S. Pui, T. Bansal, P. Kongsuphol and S. K. Arya, in *Proceedings of World Academy of Science, Engineering and Technology*, World Academy of Science, Engineering and Technology, 2012.

11 Y.-S. Fang, X.-J. Huang, L.-S. Wang and J.-F. Wang, *Biosens. Bioelectron.*, 2015, **64**, 324–332.

12 H. D. Jang, S. K. Kim, H. Chang and J.-W. Choi, *Biosens. Bioelectron.*, 2015, **63**, 546–551.

13 C.-M. Mihailescu, D. Stan, R. Iosub, C. Moldovan and M. Savin, *Talanta*, 2015, **132**, 37–43.

14 J. Liu, J. Wang, T. Wang, D. Li, F. Xi, J. Wang and E. Wang, *Biosens. Bioelectron.*, 2015, **65**, 281–286.

15 K. Omidfar, H. Zarei, F. Gholizadeh and B. Larijani, *Anal. Biochem.*, 2012, **421**, 649–656.

16 A. Ramanavicius, Y. Oztekin and A. Ramanaviciene, *Sensors Actuators B Chem.*, 2014, **197**, 237–243.

17 A. Ramanaviciene, A. Ramanavicius and A. Finkelsteinas, *J. Chem. Educ.*, 2006, **83**, 1212.

18 C.-C. Lin, Y.-M. Chu and H.-C. Chang, *Sensors Actuators B Chem.*, 2013, **187**, 533–539.

19 L. Liu, Y. Chao, W. Cao, Y. Wang, C. Luo, X. Pang, D. Fan and Q. Wei, *Anal. Chim. Acta*, 2014, **847**, 29–36.

20 Z. Taleat, A. Ravalli, M. Mazloum-Ardakani and G. Marrazza, *Electroanalysis*, 2013, **25**, 269–277.

21 Y. Zheng, Y. Yuan, Y. Chai and R. Yuan, *Biosens. Bioelectron.*, 2015, **66**, 585–589.

22 F. Li, L. Jiang, J. Han, Q. Liu, Y. Dong, Y. Li and Q. Wei, *RSC Adv.*, 2015, **5**, 19961–19969.

23 M.-C. Tu, H.-Y. Chen, Y. Wang, S. M. Moochhala, P. Alagappan and B. Liedberg, *Anal. Chim. Acta*, 2015, **853**, 228–233.

24 M. Mazloum-Ardakani and A. Khoshroo, *Electrochim. Acta*, 2014, **130**, 634–641.

25 P. Yáñez-Sedeño, J. M. Pingarrón, J. Riu and F. X. Rius, *TrAC Trends Anal. Chem.*, 2010, **29**, 939–953.

26 P. Boomi, H. G. Prabu and J. Mathiyarasu, *Colloids Surfaces B Biointerfaces*, 2013, **103**, 9–14.

27 S. Yu, Q. Lou, K. Han, Z. Wang and H. Zhu, *Int. J. Hydrogen Energy*, 2012, **37**, 13365–13370.

28 L. Li, M. Chen, G. Huang, N. Yang, L. Zhang, H. Wang, Y. Liu, W. Wang and J. Gao, *J. Power Sources*, 2014, **263**, 13–21.

29 D.-D. La, C. K. Kim, T. S. Jun, Y. Jung, G. H. Seong, J. Choo and Y. S. Kim, *Sensors Actuators B Chem.*, 2011, **155**, 191–198.

30 Z. Li, L. Fan, T. Zhang and K. Li, *J. Hazard. Mater.*, 2011, **187**, 466–472.

31 R. Wang, H. Li, H. Feng, H. Wang and Z. Lei, *J. Power Sources*, 2010, **195**, 1099–1102.

32 Y. Li, Q. Lu, S. Wu, L. Wang and X. Shi, *Biosens. Bioelectron.*, 2013, **41**, 576–581.

33 G. Wang, X. Gang, X. Zhou, G. Zhang, H. Huang, X. Zhang and L. Wang, *Talanta*, 2013, **103**, 75–80.

34 M. Du, T. Yang, S. Ma, C. Zhao and K. Jiao, *Anal. Chim. Acta*, 2011, **690**, 169–174.

35 S. Mandal, D. Roy, R. V Chaudhari and M. Sastry, *Chem. Mater.*, 2004, **16**, 3714–3724.

36 M. Mazloum-Ardakani and A. Khoshroo, *Electrochim. Acta*, 2013, **103**, 77–84.

37 A. J. Bard and L. R. Faulkner, *Electrochemical Methods: Fundamentals and Applications*, Wiley, 2nd edn., 2000.

38 M. Mazloum-ardakani and A. Khoshroo, *Anal. Chim. Acta*, 2013, **798**, 25–32.

39 A. Ramanavicius, A. Finkelsteinas, H. Cesiulis and A. Ramanaviciene, *Bioelectrochemistry*, 2010, **79**, 11–16.

Figure captions:

Scheme 1 Procedures for the preparation of TNF-α immunosensor based on Ag@Pt-CNTs/CS modified SPE.

Fig. 1 (A) UV-vis absorption spectra of Ag nanoparticles synthesized in the absence and presence of MWCNTs and MWCNTs alone. (B) TEM image of Ag@Pt-CNTs.

Fig. 2 Cyclic voltammograms of (a) Bare SPE; (b) SPE/CNTs/CS; (c) SPE/Ag@Pt-CNTs/CS; (d) SPE/Ag@Pt-CNTs/CS/Ab and (e) proposed immunosensor incubated with 15 pg/mL TNF-α in 0.1 M PBS (pH=7.4) containing 1.0 mM catechol. (f) Bare SPE; (g) SPE/Ag@Pt-CNTs/CS in 0.1 M PBS (pH=7.4). Scan rate is 100 mV/s.

Fig. 3 Nyquist plots of: (a) Bare SPE; (b) SPE/CNTs/CS; (c) SPE/Ag@Pt-CNTs/CS; (d) SPE/Ag@Pt-CNTs/CS/Ab and (e) proposed immunosensor incubated with 15 pg/mL TNF-α in in 0.1 M PBS (pH=7.4) containing 0.1 M KCl and 10 mM $[Fe(CN)_6]^{3-/4}$.

Fig. 4 DPV responses of the immunosensor to 0.1 M PBS (pH=7.4) containing 1.0 mM catechol for the detection of different concentrations of TNF-α. The numbers of a–f correspond to: 0.0, 6.0, 15.0, 30.0, 45.0 and 60.0 pg mL^{-1}, respectively. The inset is the calibration curve. Each point was repeated at least 6 times using different modified SPE.

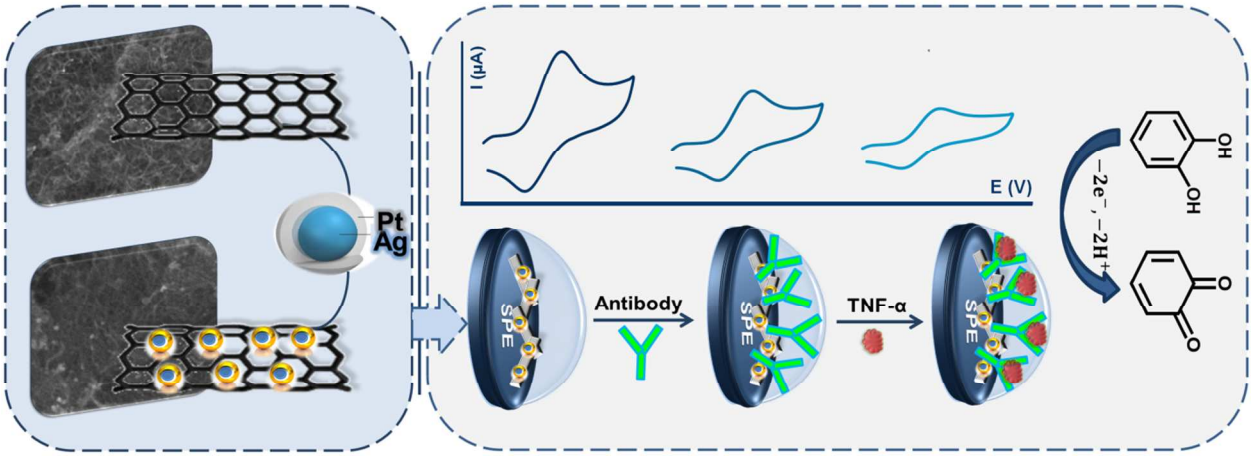

Scheme 1

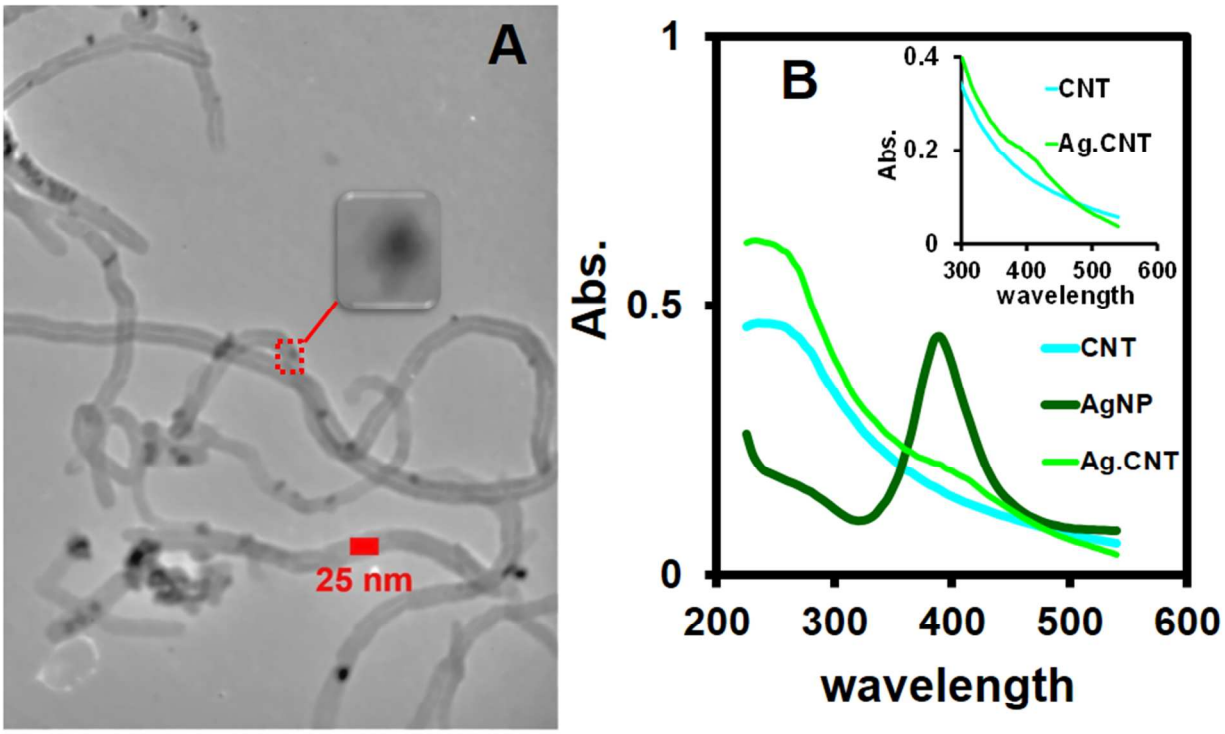

Fig. 1

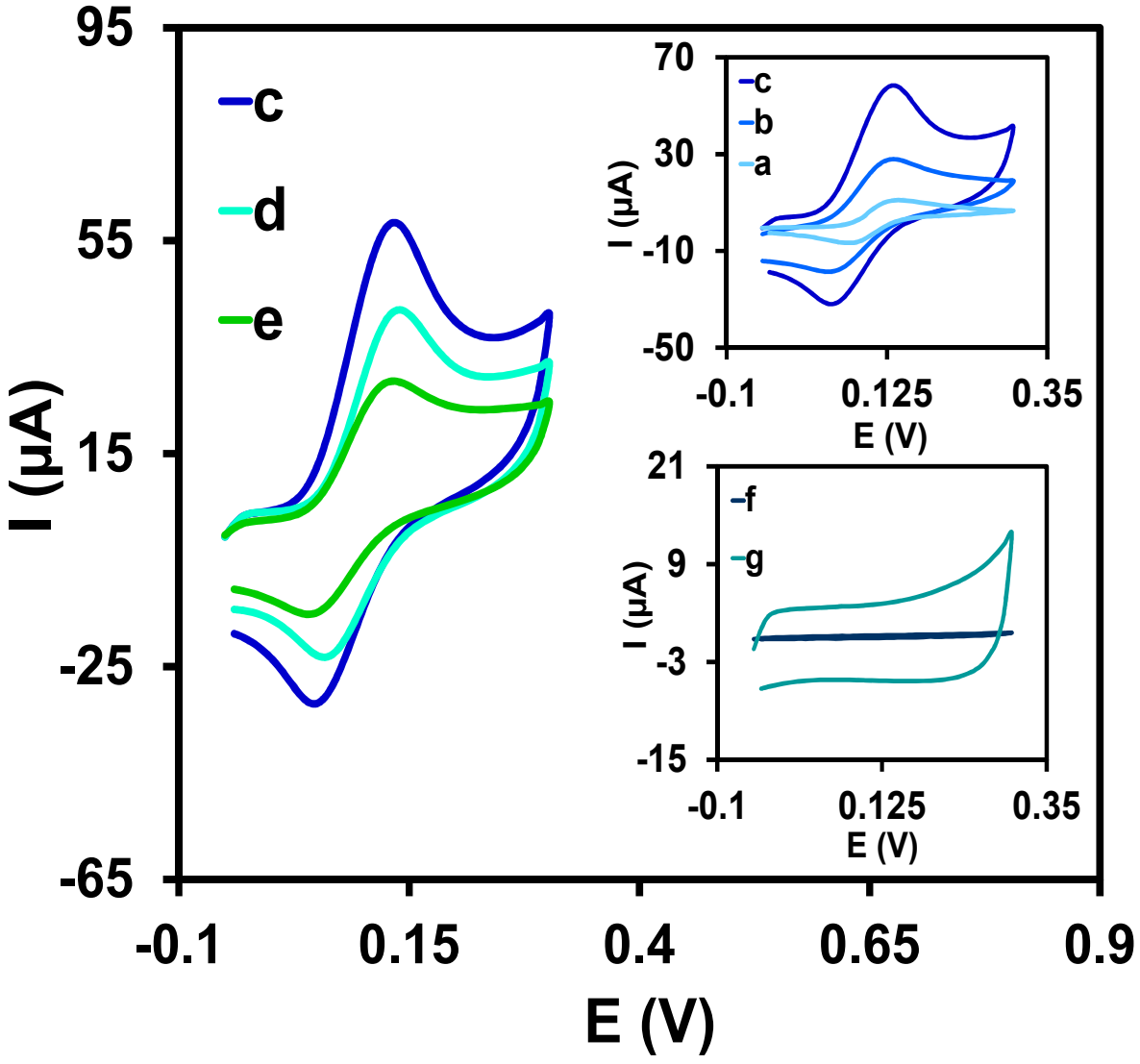
95
55
15
-25
-65
I (μA)
-0.1
0.15
0.4
0.65
0.9
E (V)
c
d
e
70
30
-10
-50
I (μA)
c
b
a
-0.1
0.125
0.35
E (V)
21
9
-3
-15
I (μA)
f
g
-0.1
0.125
0.35
E (V)

Fig. 2

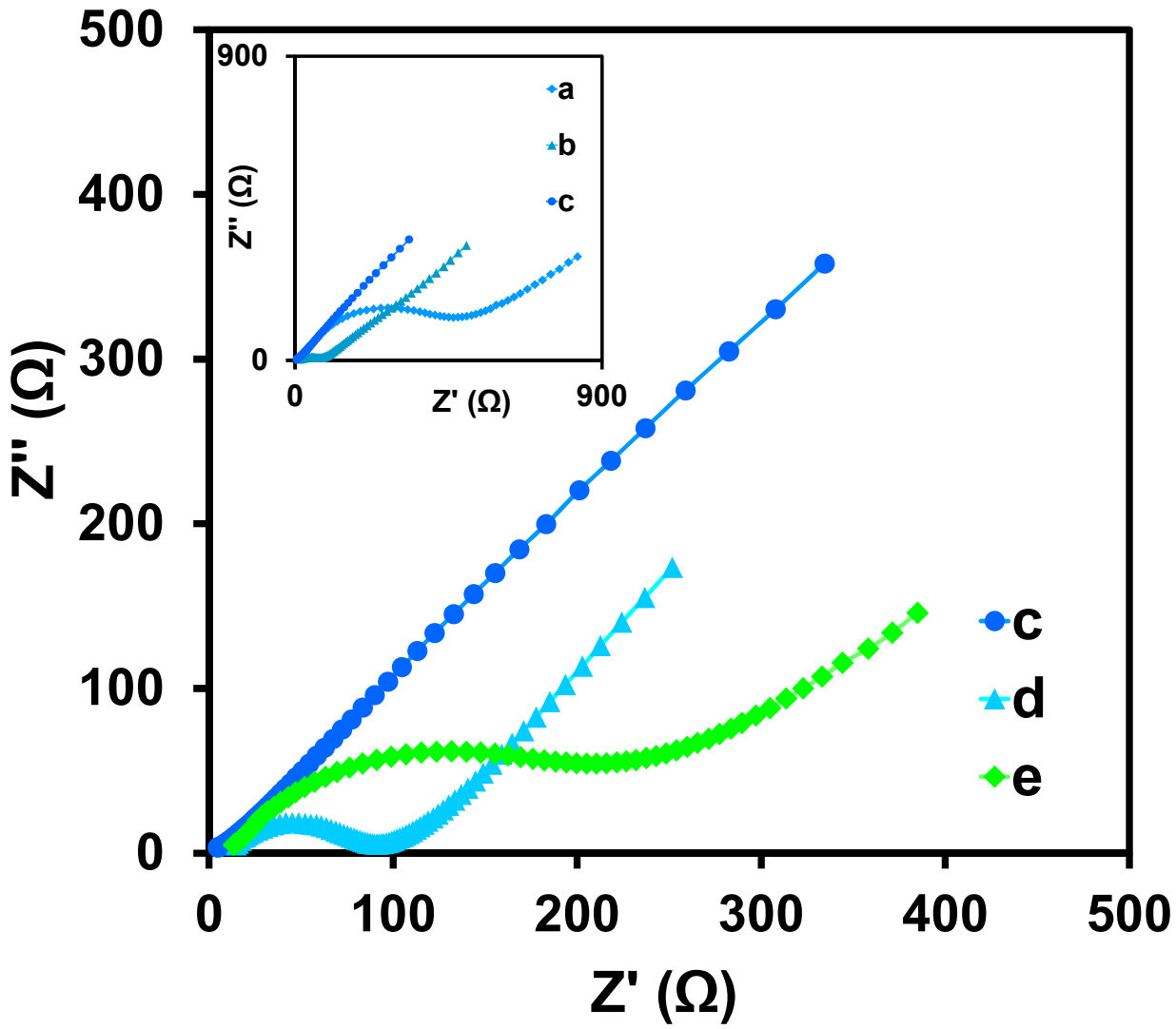
500
400
300
200
100
0
Z'' (Ω)
0
100
200
300
400
500
Z' (Ω)
c
d
e
900
0
Z'' (Ω)
0
Z' (Ω)
900
a
b
c

Fig. 3

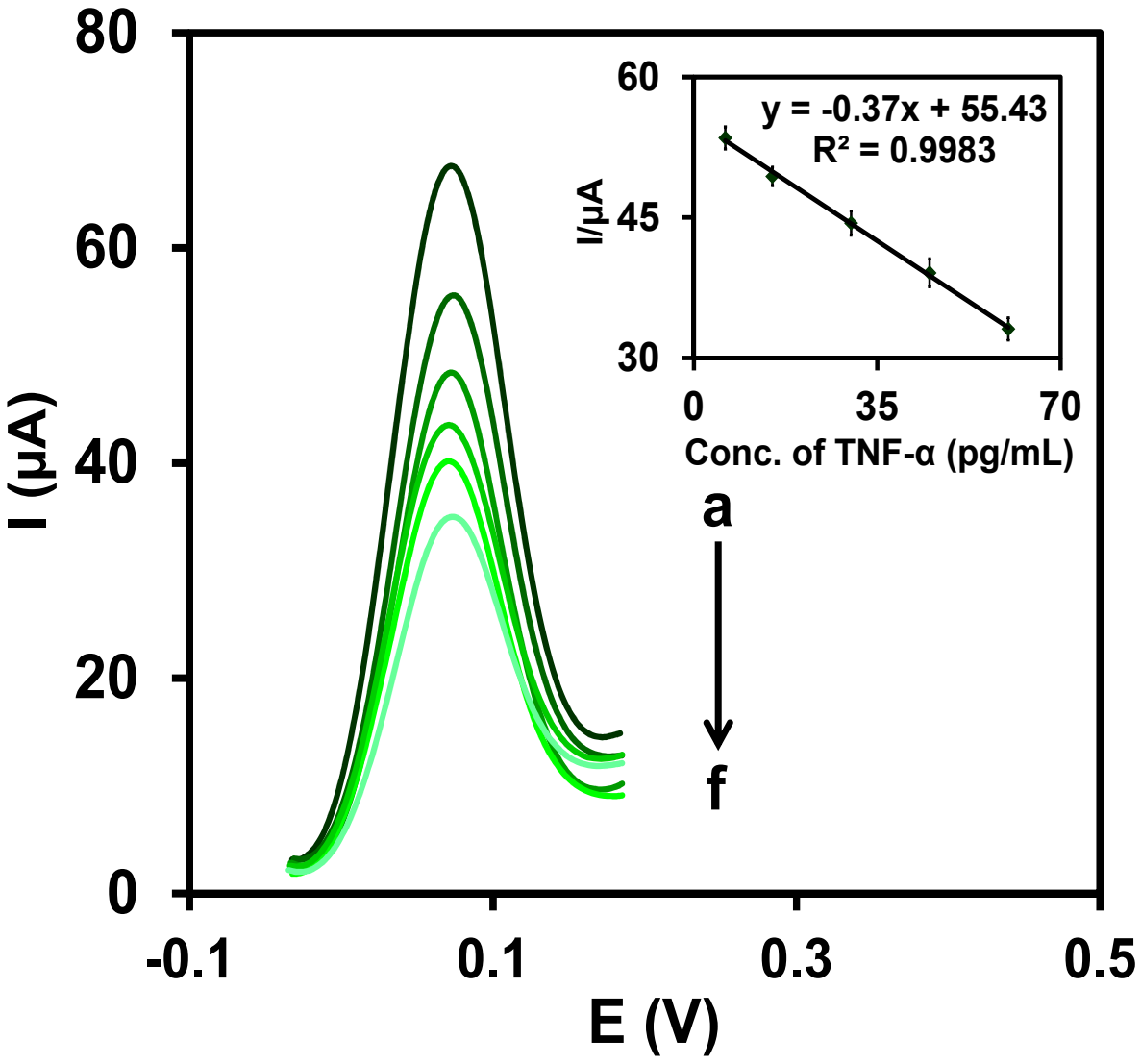
80
60
40
20
0
I (μA)
-0.1
0.1
0.3
0.5
E (V)
a
f
60
45
30
I/μA
y = -0.37x + 55.43
R² = 0.9983
0
35
70
Conc. of TNF-α (pg/mL)

Fig. 4

Table 1. Recovery of TNF-α from serum samples (pg mL^{-1}).

Sample number	1	2	3
Amount of TNF-α added	5.0	15.0	60.0
Amount of TNF-α detected	5.1	14.8	60.3
Recovery (%)	98.0	101.3	99.5
RSD (%)	3.4	3.1	2.9

Graphical abstract

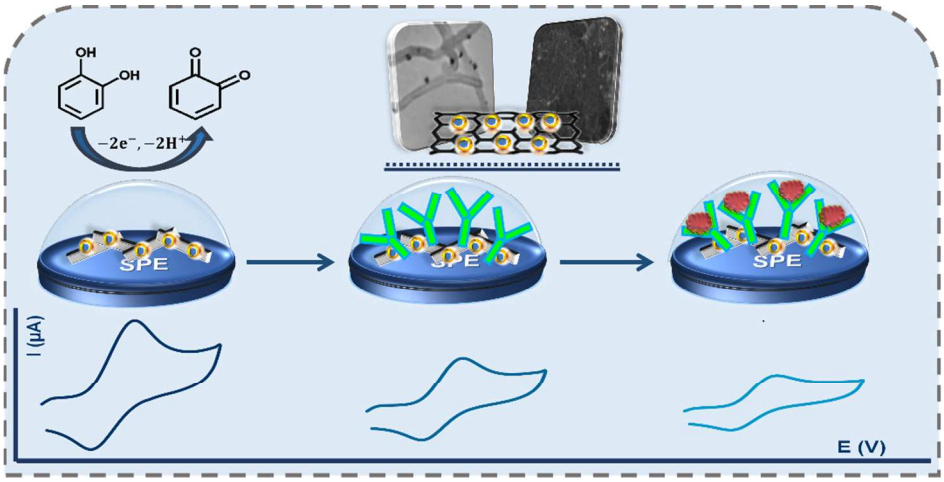

Novel label-free electrochemical immunosensors for enzyme-free determination of TNF-α was fabricated by Ag@Pt core-shell supported on MWCNTs as desirable platform.